

Hole dispersions in the *G*- and *C*-type orbital ordering backgrounds: Doped manganese oxides

Xiao-Juan Fan,^{1,2} Shun-Qing Shen,¹ Z. D. Wang,¹ X.-G. Li,² and Qiang-Hua Wang³

¹*Department of Physics, The University of Hong Kong, Pokfulam Road, Hong Kong, China*

²*Department of Materials Science and Engineering, and Structure Research Laboratory, The University of Science and Technology of China, Hefei, 230026, China*

³*Department of Physics and National Laboratory of Solid State Microstructure, Nanjing University, Nanjing 210093, China*

(Received 11 November 1999)

In the framework of the linear spin-wave theory and orbital-charge separation, we calculate quasiparticle (QP) dispersions for two different antiferromagnetic orbital structures in the fully saturated spin phase of manganese oxides. Although with the same orbital wave excitations, the QP bands of *C*- and *G*-type orbital structures exhibit completely different shapes. The pseudogap observed in the density of states and spectral functions around $\omega=0$ is related with the large antiferromagnetic orbital fluctuation. The minimal band energy for *G*-type is lower than that for *C*-type orbital order, while these band curves almost coincide in some momentum points. Larger energy splitting occurs between the two branches of $k_z=0$ and $k_z=\pi$ when increasing the superexchange coupling J , suggesting that the orbital scattering plays an essential role in the QP dispersions.

Hole-doped manganese oxides with perovskite structure exhibit rich physical behaviors, which originate from the interplay between spin, charge, orbital, and lattice degrees of freedom as well as strong correlations among electrons.^{1,2} The parent compound LaMnO_3 is an *A*-type antiferromagnetic (AF) insulator. Upon doping of holes, a ferromagnetic metallic state appears at low temperatures and the colossal magnetoresistance effect is observed near the ferromagnetic transition temperature. With dopant increasing, the ferromagnetic transition temperature decreases and an insulating state comes out again.^{3,4} Owing to the Jahn-Teller distortion, it is considered that Mn $d_{3z^2-r^2}$ and $d_{x^2-y^2}$ orbitals are alternately ordered in the crystal.⁵ The *A*-type spin and *C*-type orbital antiferromagnetic structure was observed experimentally in the undoped manganites.⁶ Recently, much attention has been attracted to the anomalous properties of $\text{La}_{1-x}\text{Sr}_x\text{MnO}_3$ at $x\sim 0.12$; the resistivity shows a sharp upturn below a certain low temperature T_{oo} .^{7,8} The ferromagnetic metal-insulator transition is actually driven by orbital ordering which was directly observed by the resonant x-ray scattering.^{6,9} The high-energy resolution angle-resolved photoemission (ARPES) measurements reveal the existence of a pseudogap (PG) at the Fermi surface¹⁰ at low temperatures. The doping induced transition to ferromagnetic metal around T_c was explained by means of double exchange (DE) theory proposed in 1950s and 1960s.¹¹ However, this scenario is not compatible with the recent experimental discoveries, and new approaches are needed to understand the complicated behaviors. Some authors ascribe the anomalous features to the orbital dynamics,^{5,12,13} which leads to the incoherent structure of the optical conductivity. Theoretical studies show that the energies of the *C*- and *G*-type orbital structures are degenerate.^{14,15} So far, little is known about the property of doped holes in Mn oxides. We believe that the orbital model provides a good starting point for considering the dynamics of holes in the ferromagnetic spin system. In particular, it is of interest to investigate the dispersion relations of a single hole moving on the two different orbital backgrounds.

In this paper, we start with an orbital t - J Hamiltonian for manganites, and assume that electronic spins are fully saturated and will henceforth be neglected here. This model consists of hopping terms between the same and different orbitals α, β on neighbor sites and an orbital superexchange interaction, which differs from the usual t - J model as a potential candidate for the microscopic understanding of the cuprites. The t - J -like orbital Hamiltonian without the spin degrees of freedom is expressed as^{16,17}

$$H = - \sum_{ij\alpha\beta} (t_{ij}^{\alpha\beta} \tilde{c}_{i\alpha}^\dagger \tilde{c}_{j\beta} + \text{H.c.}) + J \sum_{ij} \left(\tau_i^\gamma \tau_j^\gamma - \frac{1}{4} n_i n_j \right), \quad (1)$$

where $\tilde{c}_{i\alpha}^\dagger = c_{i\alpha}^\dagger (1 - n_i)$ creates an electron at an empty site i with orbital α , for which we denote the two degenerate orbits by $\uparrow = d_{3z^2-r^2}$ and $\downarrow = d_{x^2-y^2}$, and the rest of the notation is standard. In this paper, the unit of energy will be $t=1$. The transfer integral $t_{ij}^{\alpha\beta}$ depends on the orbitals, the anisotropic transfer matrices are expressed by^{12,18}

$$t_{x/y} = t \begin{pmatrix} \frac{1}{4} & \mp \frac{\sqrt{3}}{4} \\ \mp \frac{\sqrt{3}}{4} & \frac{3}{4} \end{pmatrix}, \quad t_z = t \begin{pmatrix} 1 & 0 \\ 0 & 0 \end{pmatrix},$$

and $\tau_i^{x/y} = \frac{1}{2} (T_i^z \pm \sqrt{3} T_i^x)$, $\tau_i^z = T_i^z$ with $T_i^\alpha = \frac{1}{2} (\sigma^\alpha)_{\sigma_1, \sigma_2} c_{i\sigma_1}^\dagger c_{i\sigma_2}$, σ^α are the Pauli matrices. $\gamma (= i-j) \in \{\hat{x}, \hat{y}, \hat{z}\}$. The transfer matrices $t_{ij}^{\alpha\beta}$ allow orbital flipping while an electron hops in the x - y plane, which contrasts to the usual t - J model. The superexchange coupling constant is $J=4t^2/U$, where U is the on-site repulsion between spin-parallel e_g electrons. The present model has been studied by several authors. For example the anomalous spectral distribution in doped manganites was explained.¹⁶ At $x=0$, the optimal choice of the occupied orbitals for *G* and *C* type could be chosen by minimizing the classical energy. In order

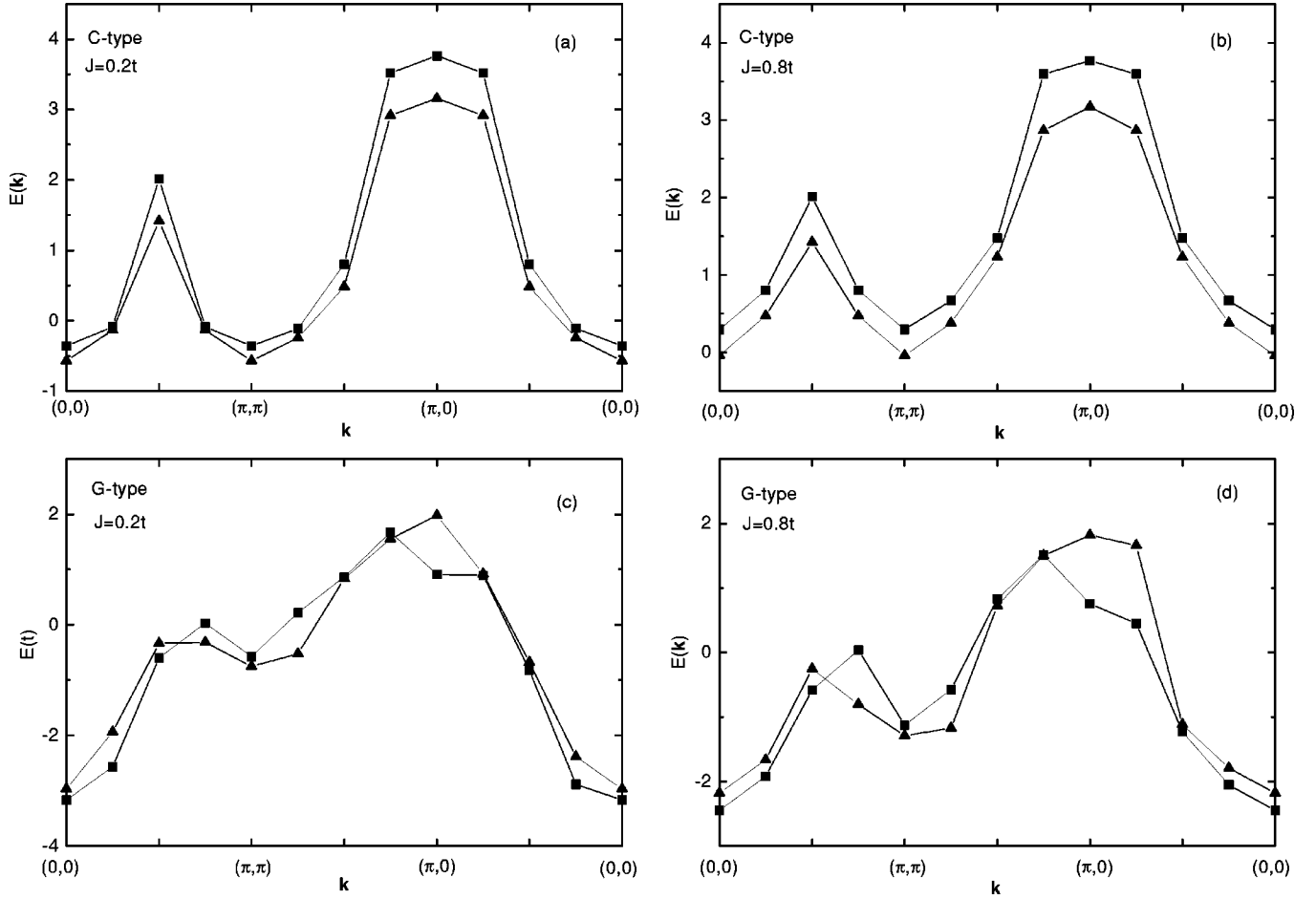


FIG. 1. Quasiparticle dispersions for G - and C -type orbital structures. The line is a guide for the eyes.

to find the optimum configuration, let us perform a uniform rotation of \uparrow and \downarrow orbitals by an angle θ at each site:

$$\begin{pmatrix} c_{\uparrow'} \\ c_{\downarrow'} \end{pmatrix} = \begin{pmatrix} \cos(\theta/2) & \sin(\theta/2) \\ -\sin(\theta/2) & \cos(\theta/2) \end{pmatrix} \begin{pmatrix} c_{\uparrow} \\ c_{\downarrow} \end{pmatrix}.$$

The value of θ is to be optimized. At $x=0$, the superexchange part H_J in the orbital subspace of Eq. (1) may be mapped onto a spin problem, and can thus be treated within the linearized spin-wave theory. Here we choose the Holstein-Primakoff transformation for localized orbital operators ($T=1/2$). $T_i^+ = a_i^+ \sqrt{1 - a_i^+ a_i}$ for $i \in A$ sublattice and $\sqrt{1 - a_i^+ a_i} a_i$ for $i \in B$ sublattice. A and B represent the different sublattices with an alternating orbital background. We find the classical ground energy depends on the rotating angle for C type but angle independent for G type. The minimum classical energy per bond is $-\frac{3}{4}J$ at $\theta = \pi/2$ for C type and at any θ for G type. In the momentum space and at $\theta = \pi/2$, the linearized Hamiltonians for G - and C -type orbital waves are identical,

$$H_J = \sum_k A_k a_k^\dagger a_k + \frac{1}{2} B_k (a_k^\dagger a_{-k}^\dagger + a_k a_{-k}), \quad (2)$$

where

$$A_k^{(1)} = 3J + B_k^{(1)}, \quad B_k^{(1)} = \frac{1}{2} J [\gamma_{\parallel}(k) + 2\gamma_{\perp}(k)]$$

and $\gamma_{\parallel}(k) = \frac{1}{2}(\cos k_x + \cos k_y)$, $\gamma_{\perp} = \cos k_z$. After a Bogoliubov transformation:

$$a_k = u_k \alpha_k + v_k \alpha_{-k}^\dagger,$$

the diagonalized orbital wave Hamiltonian takes the form

$$H_J = \sum_k \omega_k \alpha_k^\dagger \alpha_k,$$

with the orbital wave dispersion

$$\omega_k = 3J \sqrt{1 + \frac{1}{3} [\gamma_{\parallel}(k) + 2\gamma_{\perp}(k)]}.$$

This anisotropic energy of the three-dimensional (3D) model comes from the contributions of the bonds in the ab plane and along the z direction.

We assume that a slight doping does not severely disturb the long-range orbital ordering in manganites, such as C -type and G -type ordering in the undoped material LaMnO_3 . The first term H_t of Eq. (1), which describes the hopping of electrons from site to site, can be expressed in the representation of hole-orbital separation similar to the hole-spin separation for the usual t - J model in the work of Schmitt-Rink and Varma.¹⁹ This method has been widely used to describe the evolution of the quasiparticle (QP) dispersion based on the usual t - J model for cuprites.²⁰ We introduce hole operators h_i such that

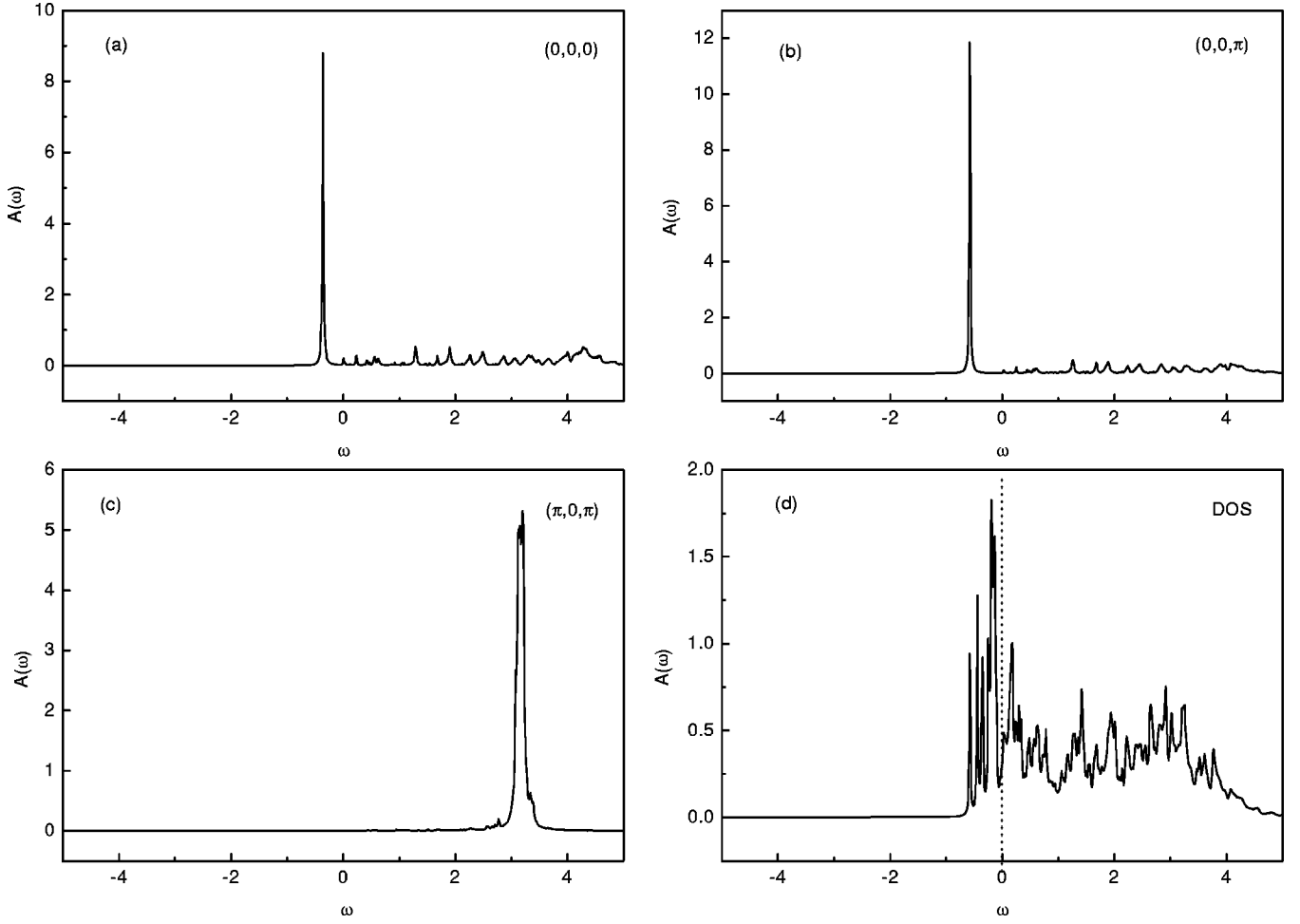


FIG. 2. Spectral functions $A(\mathbf{k}, \omega)$ for C-type orbital structure: (a) $\mathbf{k}=(0,0,0)$; (b) $\mathbf{k}=(0,0,\pi)$; (c) $\mathbf{k}=(\pi,0,\pi)$; (d) the density of states $\sum_{\mathbf{k}} A(\mathbf{k}, \omega)/N$, $J=0.2t$.

$$\tilde{c}_{i\uparrow}^{\dagger} = \begin{cases} h_i & \text{if } i \in A \\ h_i T_i^+ & \text{if } i \in B \end{cases}$$

$$\tilde{c}_{i\downarrow}^{\dagger} = \begin{cases} h_i T_i^- & \text{if } i \in A \\ h_i & \text{if } i \in B. \end{cases}$$

$$\epsilon_k^{(1)} = -t \left(\frac{\sqrt{3}}{2} (\cos k_x - \cos k_y) - 2 \cos k_z \right),$$

$$\epsilon_k^{(2)} = -\frac{\sqrt{3}}{2} t [\cos k_x - \cos k_y],$$

and

$$\xi_k^{(1)} = 2t \gamma_{\parallel}(k),$$

$$\xi_k^{(2)} = t[2\gamma_{\parallel}(k) + \gamma_{\perp}(k)],$$

$$M_{kq}^{(i)} = \frac{1}{\sqrt{N}} (\xi_k^{(i)} u_q + \xi_{k-q}^{(i)} v_q),$$

$$g_{kpq}^{(i)} = \frac{1}{N} (\epsilon_{k+p}^{(i)} u_p u_{p+q} + \epsilon_{k-p-q}^{(i)} v_p v_{p+q}),$$

$$g'_{kpq}{}^{(i)} = \frac{1}{N} \epsilon_{k+p}^{(i)} u_p v_{p+q},$$

$$g''_{kpq}{}^{(i)} = \frac{1}{N} \epsilon_{k+p-q}^{(i)} v_p u_{p+q},$$

In this representation, the Hamiltonian is reduced to

$$\begin{aligned} H^{(i)} = & \sum_{\mathbf{k}} \epsilon_{\mathbf{k}}^{(i)} h_{\mathbf{k}}^{\dagger} h_{\mathbf{k}} + \sum_{\mathbf{k}} \omega_{\mathbf{k}} \alpha_{\mathbf{k}}^{\dagger} \alpha_{\mathbf{k}} \\ & + \sum_{kq} (M_{kq}^{(i)} h_{\mathbf{k}}^{\dagger} h_{\mathbf{k}-q} \alpha_q + \text{H.c.}) \\ & + \sum_{kpq} g_{kpq}^{(i)} h_{\mathbf{k}}^{\dagger} h_{\mathbf{k}-q} \alpha_p^{\dagger} \alpha_{p+q} \\ & + \sum_{kpq} g'_{kpq}{}^{(i)} h_{\mathbf{k}}^{\dagger} h_{\mathbf{k}-q} \alpha_p^{\dagger} \alpha_{-(p+q)} \\ & + \sum_{kpq} g''_{kpq}{}^{(i)} h_{\mathbf{k}}^{\dagger} h_{\mathbf{k}+q} \alpha_p \alpha_{-(p+q)}, \end{aligned}$$

where

where $i=1,2$ for G- and C-type orbital structures.

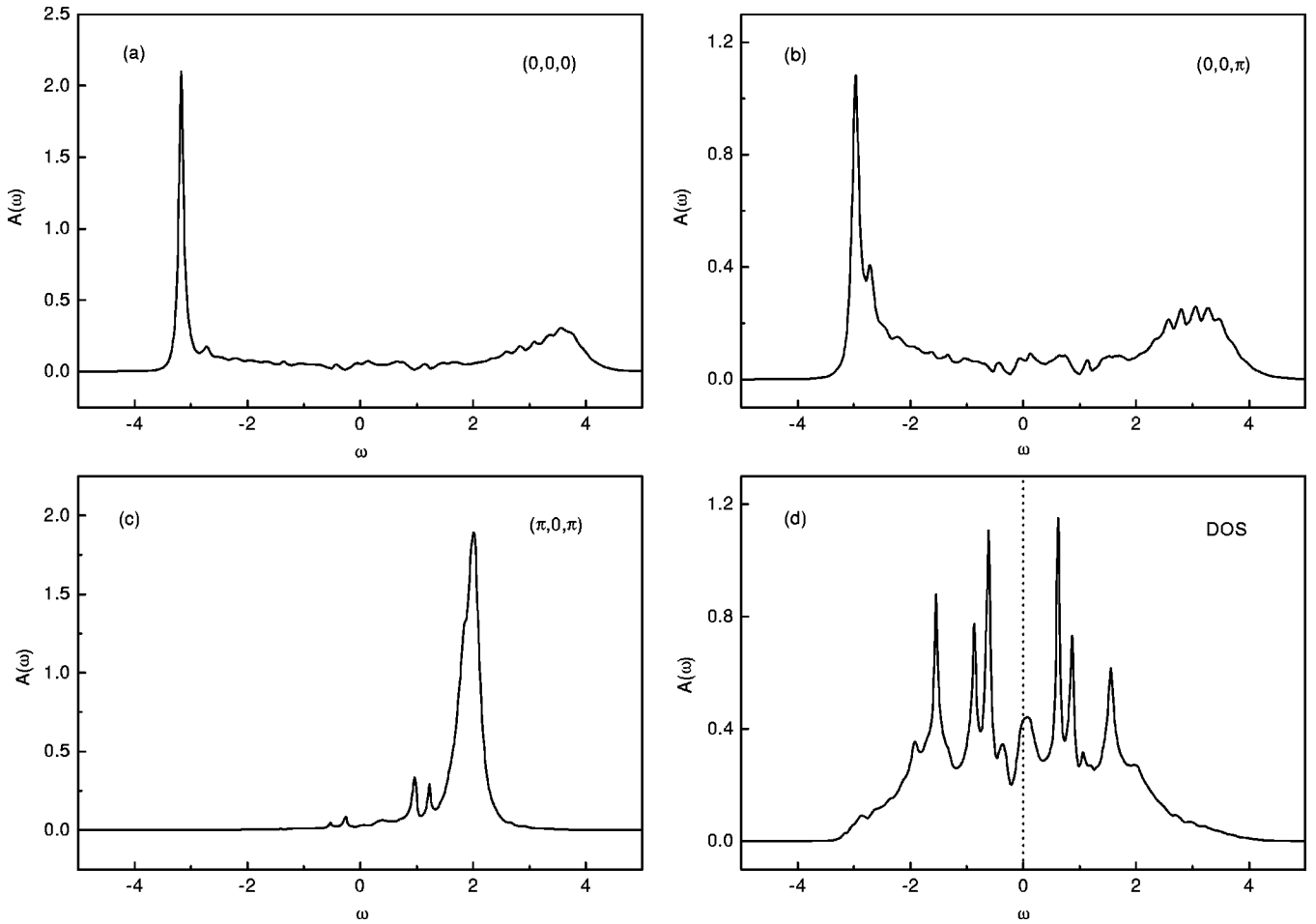


FIG. 3. Spectral functions $A(\mathbf{k}, \omega)$ for G -type orbital structure: (a) $\mathbf{k}=(0,0,0)$; (b) $\mathbf{k}=(0,0,\pi)$; (c) $\mathbf{k}=(\pi,0,\pi)$; (d) the density of states $\sum_{\mathbf{k}} A(\mathbf{k}, \omega)/N$, $J=0.2t$.

Early results for usual t - J model^{20–24} revealed that the self-consistent Born approximation presented a remarkable agreement with the exact diagonalization calculation. Based on the self-consistent diagrammatic approach, we evaluate the self-energy of these two systems numerically by the ordinary iteration procedure and in the ω mesh with 1000 points in the range from -5 to 5 (in units of t). The simulations have been carried out on clusters with $4 \times 4 \times 2$, $6 \times 6 \times 2$, and up to $8 \times 8 \times 2$ sites, and found that the finite-size effects are not expected to change the results drastically. A similar effect was also observed in the calculation in the t - J model, which the technique was first invented for. The dressed hole QP dispersion can be obtained from the poles of the hole Green's function which correspond to the maximum peak in the spectral function $A(k, \omega)$. In Fig. 1, we show the QP bands along a specific moment route in the Brillouin zone for G - and C -type orbital backgrounds. Although they have the degenerated orbital wave excitation, the holon dispersions have completely different shapes for these two backgrounds. In Fig. 1, the solid squares and up triangles correspond to the two branches of $k_z=0$ and $k_z=\pi$, respectively. It is shown that the many-body effects strongly reduce the band splitting, and the variation of two branches is very similar for each structure. The overall shape of the QP dispersion is completely different from the free hole dispersion,

which is due to the scattering of orbital in the strongly correlated system. It also differs from the usual t - J model²⁰ which has the minimum energy at $(\pi/2, \pi/2)$ and an extended “flat” region around $(\pi, 0)$. This difference originates from the interorbital flipping in the ab plane in the present model. For C -type, in Figs. 1(a) and 1(b), we find a large excitation energy around $(\pi, 0)$ comparable to the minimum value at $(0, 0)$ and (π, π) , and there is an orbital “bag” around the point (π, π) . For G type in Figs. 1(c) and 1(d), the difference between the two branches of the band is more prominent. By setting the hopping term $t=0.36$ eV consistent with band-structure calculations, we find the bandwidth of the present model is in the interval of 1.0 – 1.7 eV which is approximately in magnitude agreement to the experimental result of 1.2 eV in the angle-resolved photoemission spectroscopy for the layered manganese oxide.¹⁰ It supports the present model to describe the ferromagnetic doped manganite. On the other hand, from this picture one can see that the shape of the QP dispersion is sensitive to the coupling J , which reveals that the orbital scattering has large influence on the motion of holes. The results of spectral functions for C type are shown in Fig. 2. The quasiparticle peak is dominant at the low-energy regime. The correspondence QP energy of $k=(0,0,0)$ spectrum is slightly different from that of

$k=(0,0,\pi)$, and in (c) the spectral weight is largely reduced at $(\pi,0,\pi)$ compared to that of $(0,0,0)$ by raising the hole energy dramatically. The absence of energy weight displayed in the density of states (DOS) in Fig. 2(d) may reveal the existence of pseudogap. It also shows that a large weight accumulates around the bottom of the band. The location of the pseudogap is different from the result of the experiment,¹⁰ in which pseudogap is at the chemical potential. The difference comes from that we take the chemical potential $\mu=0$, as our calculation is limited in a finite-size system with definite number of particles. Predominantly, the PG feature is presented around $\omega=0$ in the density of states (DOS). As a comparison, the results for *G*-type structure are shown in Fig. 3. One can see that both the spectral functions and the DOS indicate the pseudogap around $\omega=0$, which is correlated with the large antiferromagnetic orbital fluctuation in this model. At $(0,0,0)$ and $(0,0,\pi)$, $A(\mathbf{k},\omega)$ has a well-defined QP peak and a part of incoherent excitations. The density of states is completely different from that of *C* type due to their different free hole dispersions and \mathbf{k} dependence couplings between holon and orbital wave. In Fig. 4, we compare the two dispersions for *G*- and *C*-type ordering at $J=0.2t$. It shows that the energy for the two types of ordering are almost degenerated around (π,π) , while in many other momenta the energy for *G* type is lower than that of *C* type, which indicates that for the ferromagnetic spin structure the *G*-type ordering may be optimal which is in agreement with the previous investigations.^{16,25} An interesting aspect of such system is that the elementary excitations have mixed orbital-hole coupling, which gives large quantum fluctuation correction to the antiferromagnetic orbital phase. We expect that the different dispersions of *C*- and *G*-type orbital backgrounds may manifest themselves in the optical conductivity, and other observable that are strongly related to elementary excitations and the quantum fluctuation effects in the manganite systems.

In conclusion, we have investigated the QP dispersion for a fully saturated spin and lightly doped manganite system.

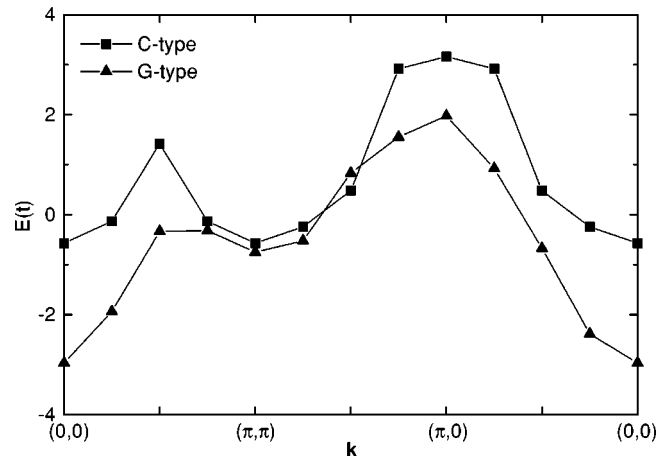


FIG. 4. Quasiparticle dispersions for *C*- and *G*-type orbital backgrounds at $J=0.2t$.

The effective Hamiltonian is derived for strongly correlated QP system with hole-orbital scattering. Based on the different *G*- and *C*-type ordering backgrounds, the hole dispersion exhibits completely different shapes, and lower energy is obtained on *G*-type orbital structure. The splitting between the two bands at $k_z=0$ and $k_z=\pi$ becomes larger upon increasing superexchange coupling. The pseudogap is apparently observed in the density of states and the spectral functions in specific moment points, which is explained by the correlation of antiferromagnetic orbital fluctuation. We believe that many anomalous properties of manganites are expected to be related to the orbital ordering. In this respect, our investigation of QP dispersion may be a prerequisite for a better understanding of the anomalous properties in the FM phase of doped manganites.

We would like to thank R.Y. Gu for helpful discussions. This work was supported by a CRCG/URC grant from the University of Hong Kong and the National Natural Science Foundation of China.

¹C.N.R. Rao and B. Raveau, *Colossal Magnetoresistance Charge Ordering and Related Properties of Manganese Oxides* (World Scientific, Singapore, 1998).

²A.P. Ramirez, *J. Phys.: Condens. Matter* **9**, 8171 (1997).

³E.O. Wollan and W.C. Koehler, *Phys. Rev.* **100**, 545 (1955).

⁴J.B. Goodenough, *Phys. Rev.* **100**, 564 (1955); in *Progress in Solid State Chemistry*, edited by H. Reiss (Pergamon, London, 1971), Vol. 5.

⁵S. Ishihara, J. Inoue, and S. Maekawa, *Phys. Rev. B* **55**, 8280 (1997); S. Ishihara, M. Yamanaka, and N. Nagaosa, *ibid.* **56**, 686 (1997).

⁶Y. Murakami, H. Kawada, H. Kawata, M. Tanaka, T. Arima, Y. Moritomo, and Y. Tokura, *Phys. Rev. Lett.* **80**, 1932 (1998); Y. Murakami, J.P. Hill, D. Gibbs, M. Blume, I. Koyama, M. Tanaka, H. Kawata, T. Arima, Y. Tokura, K. Hirota, and Y. Endoh, *ibid.* **81**, 582 (1998).

⁷S. Uhlenbruck, R. Teipen, R. Klingeler, B. Buchner, O. Friedt, M. Hucker, H. Kierspel, T. Niemoller, L. Pinsard, A. Revcolevschi, and R. Gross, *Phys. Rev. Lett.* **82**, 185 (1999).

⁸Y. Endoh, K. Hirota, S. Ishihara, S. Okamoto, Y. Murakami, A. Nishizawa, T. Fukuda, H. Kimura, H. Nojiri, K. Kaneko, and S. Maekawa, *Phys. Rev. Lett.* **82**, 4328 (1999).

⁹S. Ishihara and S. Maekawa, *Phys. Rev. Lett.* **80**, 3799 (1998); *Phys. Rev. B* **58**, 13 442 (1998).

¹⁰D.S. Dessau, T. Saitoh, C.-H. Park, Z.-X. Shen, P. Vilella, N. Hamada, Y. Moritomo, and Y. Tokura, *Phys. Rev. Lett.* **81**, 192 (1998).

¹¹C. Zener, *Phys. Rev.* **82**, 403 (1951); P.W. Anderson and H. Hasegawa, *ibid.* **100**, 675 (1955).

¹²H. Shiba, R. Shiina, and A. Takahashi, *J. Phys. Soc. Jpn.* **66**, 941 (1997).

¹³R. Kilian and G. Khaliullin, *Phys. Rev. B* **58**, R11 841 (1998).

¹⁴T. Mizokawa and A. Fujimori, *Phys. Rev. B* **51**, 12 880 (1995); **54**, 5368 (1996).

¹⁵R.Y. Gu, S.Q. Shen, Z.D. Wang, and D.Y. Xing, *cond-mat/9908464* (unpublished).

¹⁶J. van den Brink, P. Horsch, F. Mack, and A.M. Oles, *Phys. Rev.*

- B **59**, 6795 (1999); P. Horsch, J. Jaklic, and F. Mack, *ibid.* **59**, 6217 (1999).
- ¹⁷S.Q. Shen and Z.D. Wang, Phys. Rev. B **59**, 3291 (1999); **61**, 9532 (2000).
- ¹⁸J.C. Slater and G.F. Koster, Phys. Rev. **94**, 1498 (1954).
- ¹⁹S. Schmitt-Rink, C.M. Varma, and A.E. Ruckenstein, Phys. Rev. Lett. **60**, 2793 (1988).
- ²⁰E. Dagotto, Rev. Mod. Phys. **66**, 763 (1994).
- ²¹F. Marsiglio, A.E. Ruckenstein, S. Schmitt-Rink, and C.M. Varma, Phys. Rev. B **43**, 10 882 (1991); G. Martinez and P. Horsch, *ibid.* **44**, 317 (1991); Z. Liu and E. Manousakis, *ibid.* **44**, 2414 (1991).
- ²²A. Nazarenko and E. Dagotto, Phys. Rev. B **54**, 13 158 (1996).
- ²³Wei-Guo Yin, Chang-De Gong, and P.W. Leung, Phys. Rev. Lett. **81**, 2534 (1998).
- ²⁴X.-J. Fan, W.G. Yin, C.D. Gong, and X.G. Li, Eur. Phys. J. B **13**, 5 (2000).
- ²⁵T. Hotta, S. Yunoki, M. Mayr, and E. Dagotto, Phys. Rev. B **60**, R15 009 (1999).